Modular Fluorescent-Labeled Siderophore Analogues

Raphael Nudelman,[†] Orly Ardon,[‡] Yitzhak Hadar,[‡] Yona Chen,[§] Jacqueline Libman,[†,||] and Abraham Shanzer*[,†]

Department of Organic Chemistry, Weizmann Institute of Science, Rehovot 76100, Israel, and Department of Plant Pathology and Microbiology and The Otto Warburg Center for Agricultural Biotechnology, Department of Soil and Water Sciences, The Hebrew University of Jerusalem, Faculty of Agricultural, Food and Environmental Quality Sciences, Rehovot 76100, Israel

Received September 2, 1997

Biomimetic analogues **1** of the microbial siderophore (iron carrier) ferrichrome were labeled via piperazine with various fluorescent markers at a site not interfering with iron binding or receptor recognition (compounds **10**−**12**). These iron carriers were built from a tetrahedral carbon symmetrically extended with three strands, each containing an amino acid (**G** = glycyl, **A** = alanyl, **L** = leucyl and **P** = phenylalanyl) and terminated by a hydroxamic acid, which together define an octahedral iron-binding domain. A fourth exogenous strand provided the site for connecting various fluorescent markers via a short bifunctional linker. Iron(III) titrations, along with fluorescence spectroscopy, generated quenching of fluorescence emission of some of the probes used. The quenching process fits the Perrin model which reinforces the intramolecular quenching process, postulated previously.[1] All tested compounds, regardless of their probe size, polarity, or the linker binding them to the siderophore analogue, promote growth of *Pseudomonas putida* with the same efficacy as the nonlabeled analogues **1**, with the added benefit of signaling microbial activity by fluorescence emission. All **G** derivatives of compounds **10**−**12** were found to parallel the behavior of natural ferrichrome, whereas **A** derivatives mediated only a modest iron(III) uptake by *P. putida*. Incubation of various *Pseudomonas* strains with iron(III)-loaded **G** derivatives resulted in the build-up of the labels' fluorescence in the culture medium to a much larger extent than from the corresponding **A** derivatives. The fluorescence buildup corresponds to iron utilization by the cells and the release of the fluorescent labeled desferrisiderophore from the cell to the media. The fact that the microbial activity of these compounds is not altered by attachment of various fluorescent markers via a bifunctional linker proposes their application as diagnostic tools for detecting and identifying pathogenic microorganisms.

Introduction

Iron is a trace element essential for all organisms with only a few exceptions.[2] It is required for basic cellular functions such as respiration and DNA synthesis. In aerobic environments iron exists as Fe(III) ion, forming extremely insoluble oxide and hydroxide salts (K_{sp} = 10^{-38}). Siderophores are chelating agents produced by microorganisms in iron deficient environments, which solubilize and mobilize iron into their cells by ferrisiderophore complexation.[3] Microorganisms invading the circulating blood produce siderophores which compete for iron with the human transport protein transferrin, thus constituting one aspect of virulence and pathogenicity.[4−6] In bacteria the iron uptake system is usually specific and involves a number of membranal proteins activated under iron stress.[7]

Three different iron(III) uptake mechanisms are known for siderophore-mediated iron transport across microbial cell membranes.[8] The first mechanism, which appears to be the most common one, involves a transporter or permease for intact iron(III)−siderophore complexes. The outer membrane transversing occurs via a high-affinity active transport mechanism. After transport, iron is removed from the complex, and the desferri chelate is either secreted back to the medium and possibly recycled there, or is hydrolyzed inside the cell. The other two mechanisms involve extracellular iron reduction followed by its uptake.

The extensively studied ferrichrome transporter in *Escherichia coli* is regulated by the Ton system.[7,9−11] Particular gating loops in the outer membrane were shown to be responsible for high specificity and molecular recognition.[11,12] Recently, it has been shown that gated-porin channels open and close during membrane transport.[13] It is assumed that ferrichrome uptake mechanisms for other bacteria are similar to the well-defined mechanism found in *E. coli*.

Our studies have demonstrated that synthetic ferrichrome analogues simulate natural ferrichrome as growth promoters of *P. putida*.[14] Small neutral fluorescent labels have been attached to synthetic siderophores[1,15−21] and their potential as powerful tools for iron(III) transport and uptake processes in microorganisms has been shown.[1,18−22] Moreover, some of these compounds distinguish between different *Pseudomonas* species with high specificity.[1] However, it was not clear whether fluorescent probes of substantial size and/or

* Corresponding author. Tel: +972-8-934-3954. Fax: +972-8-934-2917. E-mail: coshanzr@weizmann.weizmann.ac.il.
[†] Weizmann Institute of Science.
[‡] Department of Plant Pathology and The Otto Warburg Center for Agricultural Biotechnology, The Hebrew University of Jerusalem.
[§] Department of Soil and Water Sciences, The Hebrew University of Jerusalem.
[||] Dr. Jacqueline Libman, a main contributor to the work described in this article, passed away prematurely on March 30, 1997. This article is dedicated to her memory.

S0022-2623(97)00581-5 CCC: $15.00
Published on Web 04/14/1998

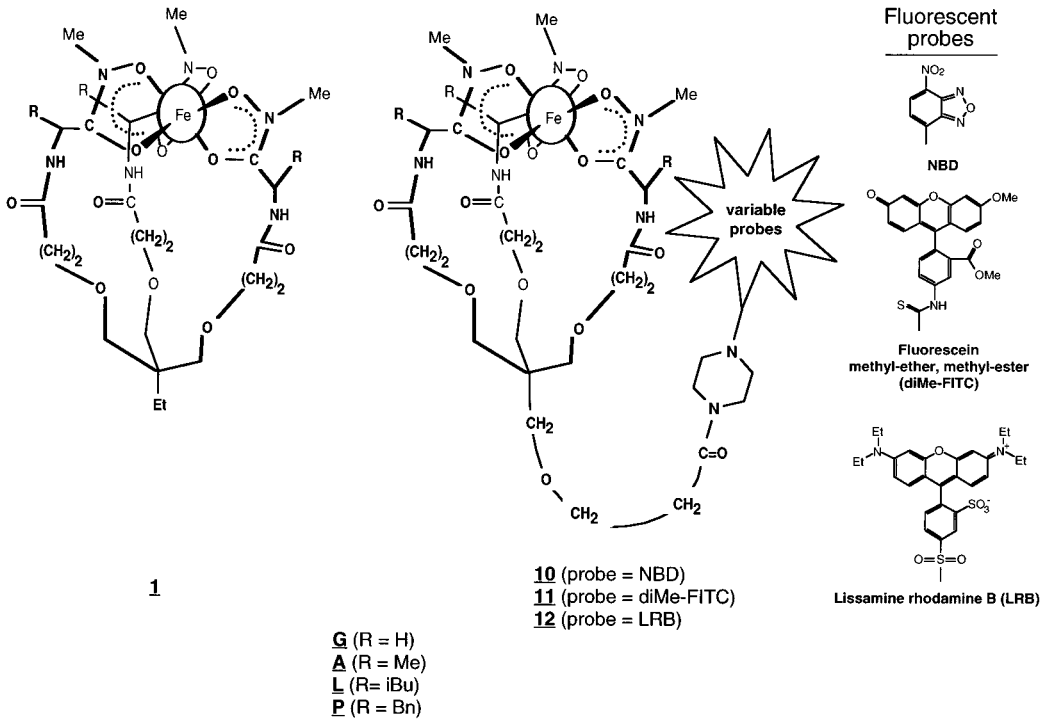

Figure 1. Schematic presentation of ferrichrome analogues **1** and fluorescent ferrichrome analogues **10**−**12**.

charge could penetrate via particular siderophore transport systems.

In this work we introduce a series of bioactive ferrichrome analogues labeled with various fluorescent probes at a site that does not interfere with iron binding or with receptor recognition. The synthetic methodology is based on piperazine as a bifunctional linker, which connects the probes to the ferrichrome analogues. We have found that in the presence of iron(III), divergent fluorescent behavior is displayed depending on the nature of the probe. Compounds **10** and **11** underwent fluorescent quenching upon iron(III) binding and regained their fluorescence upon ligand exchange with a competing chelator or via iron removal by the microbial cell. These analogues were detected in the extracellular medium as a result of microbial iron uptake. The fluorescence of compounds **12** was completely unaffected by the presence or absence of iron, thereby facilitating the monitoring of the iron uptake pathway in fungal cells.[23] All the synthesized compounds, independent of the probe's size or charge, display microbial activity in *P. putida* similar to that of the biomimetic analogues lacking the probe.

Results and Discussion

Design. A series of fluorescent ferrichrome analogues was synthesized by linking fluorescent probes to bioactive ferrichrome analogues **1**, at a site not interfering with the ferrichrome receptor binding (Figure 1).[24] The glycyl ferrichrome analogue **1G** (R = H), which fully mimics natural ferrichrome as an iron(III) carrier and growth promoter, is taken up by specific receptor recognition in *P. putida*.[14] However, the alanyl analogue **1A** (R = Me) inhibits the action of the natural iron(III) carrier by competing for a specific site in the uptake system.[14] Siderophore analogue **1A** alone promotes some growth, but at a much lower level than the natural ferrichrome or the **1G** analogue. The hydrophobic leucyl (R = *i*-Bu) and phenylalanyl (R = Bn) derivatives (**L** and **P** analogues in Figure 1), which do not promote growth,[25,26] were used as reference compounds. The **L** derivative was used in microbial iron(III) utilization studies, whereas **L** and **P** derivatives were used in fluorescence quenching measurements.

In earlier experiments it was shown that attachment of the chemically inert anthracene to the carbon anchor of ferrichrome analogues did not interfere with recognition by iron(III)−ferrichrome-specific uptake systems or with the affinity of the iron(III) binding to the siderophores.[1] Analogous compounds **10**−**12** were prepared by linking various fluorescent probes to the tetrahedral carbon of ferrichrome analogues **1**, via piperazine as a bifunctional linker. This methodology, which facilitated the insertion of a variety of fluorescent probes, enabled the selection of probes suitable for available spectroscopic devices, such as light sources and filters used in fluorescence microscopy, as well as the adaptation of commercial probes. The strategy for choosing the fluorescent probes was to determine whether characteristic structural factors such as polarity and size of the fluorescent probes effect the siderophores' cell transmembranal transport. NBD and the fluorescein derivative diMe-FITC have similar optical properties but differ in size, whereas lissamine rhodamine B (LRB) and diMe-FITC are of similar size but differ in polarity (Figure 1). Thus cell penetration characteristics of the fluorescent ferrichrome analogues, as a function of size and polarity, could be perused. The fluorescence intensity of these probes was found to be stronger than the autofluorescence of the bacterial culture. Another aspect considered in the choice of probes was the differences in their quenching properties. The fluorescence emission of NBD and of diMe-FITC are quenched in the presence of iron(III), whereas that of LRB is not. These optical properties enabled both in vitro monitoring of iron(III) binding and in vivo follow-up of the

Scheme 1. Synthesis of Fluorescent Ferrichrome Analogues

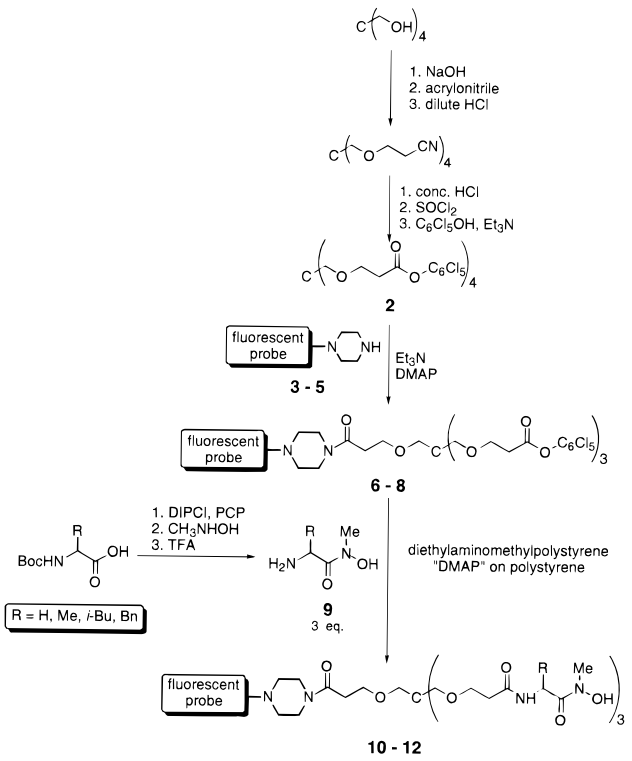

microbial iron(III) uptake process. The fate of the iron carriers after iron delivery could be monitored optically by using the quenchable probes, and the iron uptake pathway in eukaryote cells could be followed using the nonquenchable probe.[23]

Synthesis. The labeled ferrichrome analogues were prepared by coupling the C_3-symmetric tetraphenolate **2** with equivalent amounts of the piperazinyl-fluorescent probe conjugates **3**−**5**, followed by coupling with 3 equiv of hydroxamate-bearing amino acid residues **9** (Scheme 1). This two-step synthesis gave yields *significantly* higher than the one-pot reaction procedure described previously, by eliminating statistically possible byproducts.[1]

The piperazinyl-fluorescent probe conjugates were prepared by condensing NBD chloride or LRB sulfonyl chloride with piperazine, yielding monosubstituted piperazinyl-NBD **3** and piperazinyl-LRB **5**, respectively. Condensation of fluorescein-5-isothiocyanate (FITC isomer I) with *N*-*t*-Boc-piperazine followed by methylation gave the methyl ester, methyl ether of fluorescein (diMe-FITC) (Scheme 2). This alkylation, which was necessary for the purification of the compounds, reduced fluorescence intensity. (Etherification of both phenolic groups of fluorescein locks the molecule into its nonfluorescent lactone form.[27]) However, the fluorescence intensity of fluorescein's monoether derivative was found to be adequate for this work, because of its high quantum yield. Final removal of the Boc resulted in the synthesis of the desired piperazinyl-(diMe-FITC) conjugate **4**.

Iron(III) Binding Properties. Fluorescence quenching can occur by electron transfer, energy transfer, or by intersystem crossing. Earlier studies suggested that fluorescence quenching by electron transfer requires

Scheme 2. Synthesis of Piperazinyl-Fluorescent Probe Conjugates

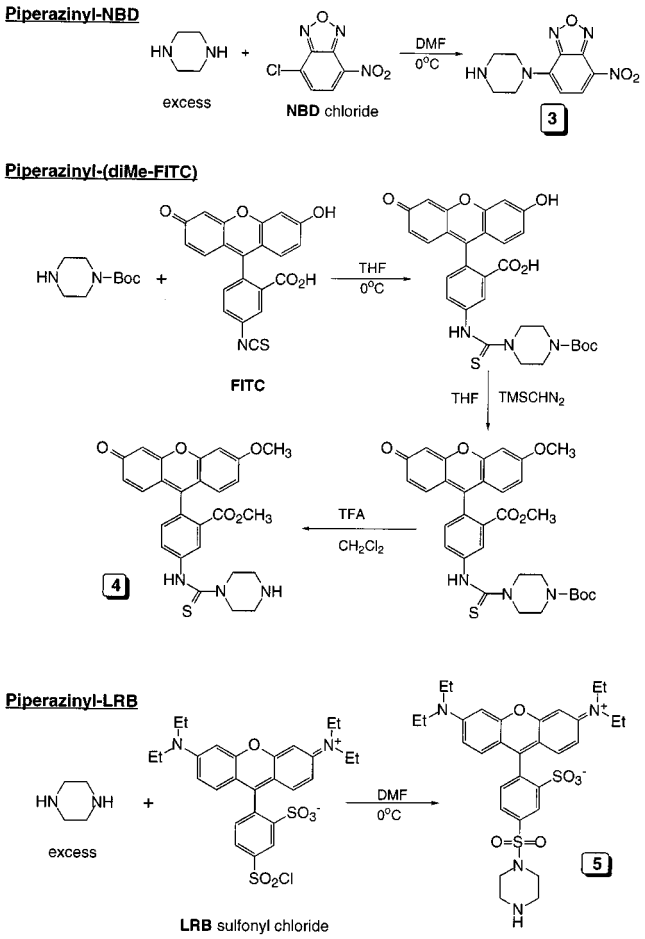

that the fluorescent probe be in proximity to its quencher (the iron binding domain in our case).[28] Indirect evidence[21,29,30] indicates that electron transfer is indeed involved in these processes. Furthermore, the diversity of spectral properties of the fluorescent probes influenced the quenching of fluorescence emission (Table 1).

Upon titration with iron(III), the fluorescence emission of the NBD derivatives **10** (Figure 2) and the diMe-FITC derivatives **11** (data not shown) was quenched.

The observed fluorescence quenching, ϕ/ϕ_o, of these ferrichrome analogues was not linear with quencher [iron(III)] concentration and thus failed to obey the Stern−Volmer model of dynamic quenching (Figure 3, top). However, the ln ϕ/ϕ_o values were linear with quencher concentration, in agreement with the Perrin model of static quenching (Figure 3, bottom), suggesting that all the added quencher is bound to the ligand, and the quenched chromophore lies within the quencher's active sphere.[31] This agreement with the Perrin model further supports the suggestion that fluorescence quenching for systems of this type occurs intramolecularly.[1]

The fluorescence quenching efficiency values of compound **10** and **11**, in the Perrin equation were $k' \approx 2 \times 10^5\ M^{-1}$ and $1 \times 10^5\ M^{-1}$, respectively. The fluorescence emission of LRB derivatives of compound **12** was not quenched at all by iron(III) chelation (data not shown). This observation implies a relationship between the optical properties of a fluorescent probe and its quenching ability.

Table 1. Spectral Characteristics of Fluorescent Ferrichrome Analogs

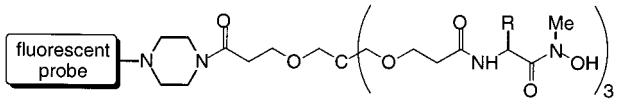

compd no.	R (amino acid derivative)	fluorescent probe	excitation (λ_{max} nm)	ϵ ($\times 10^3$ cm^2 M^{-1})	emission (λ_{max} nm)	fluorescent quenching efficiencies (k_q)
10G	H (glycyl)	NBD	474	23	540	2×10^5 M^{-1}
10A	Me (alanyl)					
10L	*i*-Bu (leucyl)					
10P	Bn (phenylalanyl)					
11G	H (glycyl)	diMe-FITC	457	25	522	1×10^5 M^{-1}
11A	Me (alanyl)					
12G	H (glycyl)	LRB	530	53	606	~0
12A	Me (alanyl)					
12L	*i*-Bu (leucyl)					

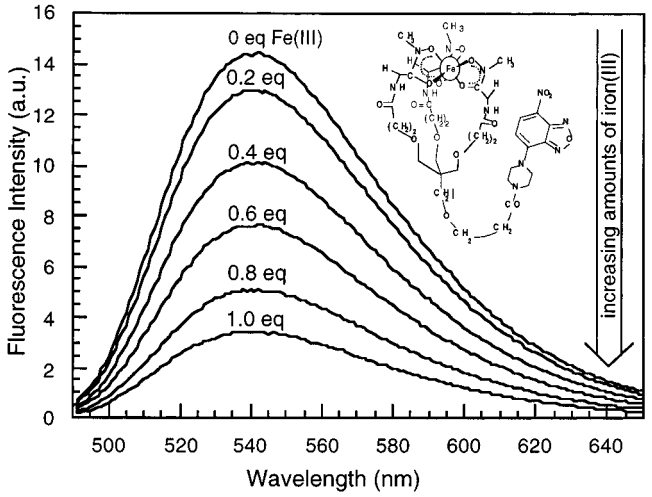

Figure 2. Fluorescence iron(III) titration curves with labeled ferrichrome analogue **10G**. Aliquots of stock solutions of **10G** in MeOH were treated with aliquots of methanolic solutions of $FeCl_3$ (0, 0.2, 0.4, 0.6, 0.8, and 1.0 equiv) and diluted with MeOH (80%)−0.1 N aqueous NaOAc (20%) to a final ligand concentration of 50 μM.

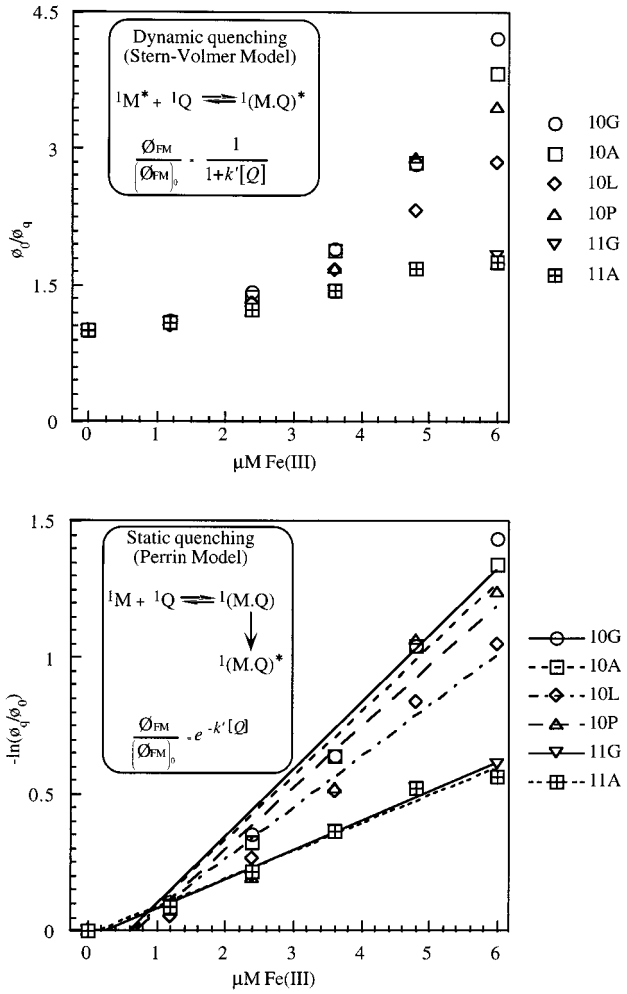

Figure 3. Plots for dynamic quenching (top) and static quenching (bottom) of the fluorescent-labeled ferrichrome analogues **10G**, **10A**, **10L**, **10P**, **11G**, and **11A** by iron(III). The conditions were as described in the legend of Figure 2.

Biology

Microbial Growth Promotion in Liquid Medium. The growth-promoting effects of iron(III)-loaded ferrichrome and its synthetic analogues were studied in liquid media. The growth was tested with *P. putida* JM218, a non-siderophore-producing mutant; therefore, no ligand exchange could occur between exogenous and native siderophores. Growth of such sid$^-$ mutants is therefore proportional to the bioavailability of the iron source supplied. Here we have shown that all **G** ferrichrome derivatives, irrespective of the size or polarity of the fluorescent probes linked to them, promoted the growth of *P. putida* with the same efficiency as the nonlabeled analogue **1G** and as the natural ferrichrome. However, all **A** derivatives promoted growth to a lesser extent than both the **G** derivatives and the natural ferrichrome, while retaining efficacy regardless of the probe attached. Figure 4 presents the growth of compounds **10G** and **10A** in comparison to ferrichrome, **1G** and **1A**. Similar results were observed for compounds **11G**, **11A**, **12G**, and **12A** (data not shown).

Microbial Iron(III) Uptake. Natural ferrichrome and its synthetic analogues are released to the culture medium after delivering iron(III) to the bacterial cells.[1] Therefore, analogues whose fluorescence was quenched by iron(III) binding regained their fluorescence and were detected in the culture medium in accordance with the microbial uptake of iron(III). *P. putida* JM218 was incubated with iron(III) complexes of **10G**, **11G**, **10A**, **11A**, and **10L**, and the appearance of the free ligands fluorescence in the growth media culture was monitored (Figure 5). The fluorescence obtained from the **G**

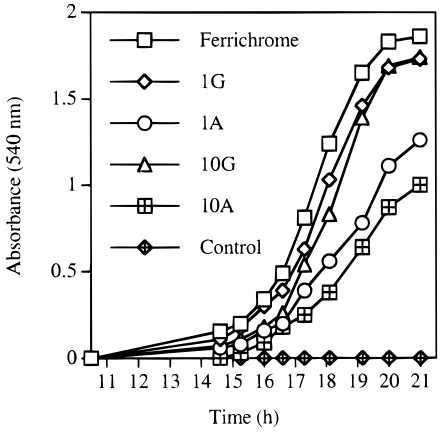

Figure 4. Growth promotion of *P. putida* JM218 in liquid medium in the presence of iron(III)-loaded ferrichrome and its synthetic analogues, **1G**, **1A**, **10G**, and **10A**.

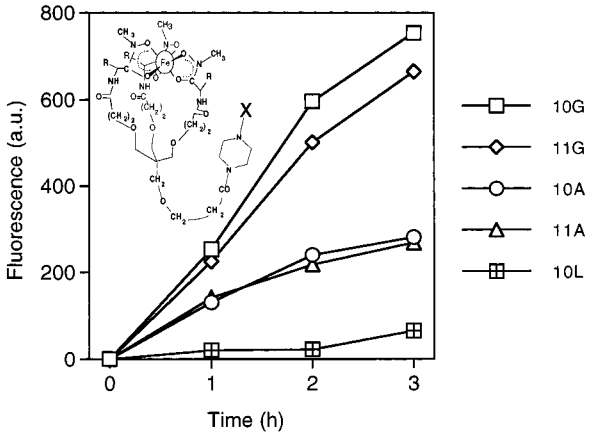

Figure 5. Emergence of fluorescence signals derived from ferrichrome analogues in cultures of *P. putida* JM218.

derivatives indicated more efficient iron(III) utilization than from the **A** analogues, whereas the lack of any fluorescence from the hydrophobic **L** derivative indicated that iron(III) was not utilized. The data were compared to that obtained from two other Pseudomonads (*Pseudomonas fluorescens* S680 and *Pseudomonas fluorescens* WCS 3742). In ferrichrome analogues where no piperazine ring linked the fluorescent probe (anthracene) to the fourth exogenous strand, selectivity was exhibited between these Pseudomonads.[1] In the present study, similar specificity toward the amino acid derivative (**G** or **A**) was observed regardless the fluorescent probe conjugated, but no selectivity was detected between the different strains (data not shown). This lack of selectivity resembles that of the natural ferrichrome's toward these Pseudomonads.[32]

Fluorescence of the nonquenchable ferrichrome analogues in the cultures' medium is obviously not an indication of iron uptake. Therefore, to show that nonquenchable analogues compete for a common receptor in the uptake system in *P. putida*, the fluorescence emission of **10G** (a quenchable ferrichrome analog) in the culture medium was measured in the presence of compounds **12G** and **12A** (nonquenchable ferrichrome analogues), and **1G** and **1A** (nonlabeled ferrichrome analogues). As predicted, **12G** and **1G** equally decreased the fluorescence emission intensity of **10G** to a larger extent than **12A** and **1A**, suggesting an inhibition of bacterial iron utilization from **10G** (Figure 6).

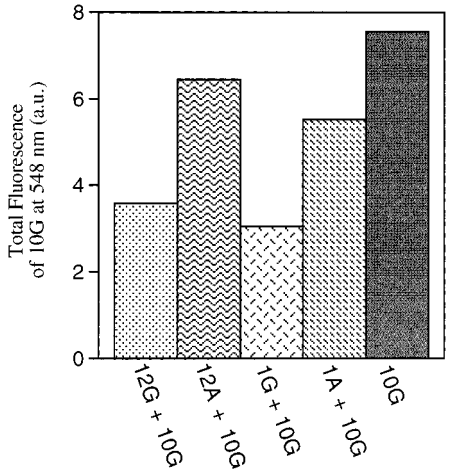

Figure 6. The fluorescence appearance in cultures of *P. putida* JM218 amended with **10G** (1 μM) in the presence of other ferrichrome analogues (1 μM).

Addition of sodium azide to the medium drastically reduced the increase of fluorescence in the supernatant as well as the ^{55}Fe(III) incorporation to the cell, indicating that iron(III) uptake in *P. putida* is an energy driven process, as shown previously.[1,14]

Our experiments indicated that neither size nor polarity of the attached fluorescent probe interferes with the recognition of the siderophore and its transport in *P. putida*. The **G** ferrichrome analogues were found to be better promoters of iron(III) uptake than the corresponding **A** analogues just as their parent nonlabeled ferrichrome analogues do.[14]

Conclusions

Biomimetic siderophore analogues were found to be useful tools for studying iron uptake in bacteria and fungi.[14,22,33−40] Attaching a fluorescent derivative to a site which does not interfere either with the recognition of the siderophore by the cell or the transport of the iron to it, enables the selection of these compounds in iron uptake studies. Earlier results[1] along with the present work demonstrated the usefulness of these novel tools in studying the ferrichrome uptake system in *Pseudomonas* sp. The possible attachment of fluorescent labels to the siderophore via short bifunctional linkers enables to choose the most suitable probe for each specific microbial system (e.g., the avoidance of autofluorescence of the cells). These modular compounds facilitate the use of different fluorescence techniques with the available laboratory equipment (e.g., different filters in fluorescent microscopes). The preferential iron uptake of microorganisms may lead to the development of species−specific libraries of siderophore analogues. The uniqueness of the compounds described herein is that they can serve as diagnostic tools for the presence of living cells and particularly pathogenic ones in a physiologically active form or stage.

Experimental Section

General Methods. Melting points were measured with a Fischer-Jones apparatus and are uncorrected. IR spectra were recorded on a Nicolet 510 FTIR spectrometer. UV/vis was measured with a Hewlett-Packard model 8450A diode array spectrophotometer. Molar extinction coefficients ϵ are given in units of cm^2 M^{-1}. Fluorescence spectra were recorded on a

SLM-AMINCO MC200 monochromator fluorospectrometer. In biological experiments fluorescence was measured with a SLM Instruments fluorometer (model 4800). ^{1}H NMR spectra were measured on a Bruker AMX-400 MHz spectrometer or on a Bruker DPX-250 MHz spectrometer with TMS as the internal reference. All *J* values are given in hertz. Positive fast atomic bombardment mass spectrometry (FABMS) was measured on a VG Autospec Fison Instruments mass spetrometer. Flash chromatography was performed using Merck 230−400 mesh silica gel. Thin-layer chromatography (TLC) on silica gel 60 F-254 on aluminum was visualized by UV light, by ninhydrin, by iodine, or by $FeCl_3$/EtOH.

Solvents and Materials. MeCN and CH_2Cl_2 were dried by filtration through basic alumina. Acrylonitrile was purified prior to use by filtration over neutral alumina. THF was distilled from Na/benzophenone under Ar. All reagents unless otherwise mentioned were purchased from Sigma and were used without further purification. Piperazine was dried under vacuum over P_2O_5. Compound **2**[1] and *N*-*t*-Boc-protected **9**[41] were prepared according to our earlier procedures. The following abbreviations have been used: DIPCI = diisopropylcarbodiimide, PCP = pentachlorophenol, pip = piperazine, NBD chloride = 4-chloro-7-nitrobenzofurazane, FITC = fluorescein isothiocyanate, LRB = lissamine rhodamine B, TMSCHN$_2$ = trimethylsilyldiazomethane.

Piperazinyl-NBD (3). A solution of NBD chloride (Fluka, 2.00 g, 10 mmol) in THF (80 mL) was slowly added to an ice cold solution of piperazine (2.68 g, 31 mmol) in THF. The color of the solution changed instantaneously to orange and within a few seconds became red. The solvent was evaporated, the crude product was dissolved in a minimal amount of MeOH/acetone (1:1), and the solution was dripped into $CHCl_3$ (500 mL). The mixture was extracted with water, dried (Na_2SO_4), and concentrated to give **3** as a red powder (2.5 g, 10 mmol, ~100% yield). ^{1}H NMR (acetone-d_6): δ 8.47, 6.63 (two d, J = 9.2, 2H, ArH), 4.16 (t, J = 5.0, 4H, CH_2NAr), 3.07 (t, J = 5.0, 4H, CH_2NH).

Piperazinyl-diMe-FITC (4). A solution of FITC isomer I 90% (400 mg, 0.924 mmol) and Boc-piperazine (172 mg, 0.924 mmol) in THF was stirred under Ar for 2 h. TMSCHN$_2$ (0.92 mL of 2.0 M solution in hexanes, 1.84 mmol) was added, and the solution was stirred overnight. The solvent was evaporated, and flash chromatography ($CHCl_3$/MeOH 98:2) of the residue provided the Boc-protected product of **4**. The Boc was removed by stirring in TFA/CH_2Cl_2 (1:2) for 20 min, the product was neutralized with [(diethylamino)methyl]polystyrene, filtered, and flash chromatographed ($CHCl_3$/MeOH 4:1), yielding **4** as a yellow waxy solid (110 mg, 0.22 mmol, 24%). ^{1}H NMR ($CDCl_3$): δ 9.84 (s, 1H, NH), 8.23 (d, J = 2.1, 1H, C*H*CCOOMe), 7.75 (dd, J_1 = 8.0, J_2 = 2.1, 1H, C*H*CNH), 7.10 (d, J = 9.1, 1H, C*H*CHCOMe), 7.09 (d, J = 8.0, 1H, C*H*CHCNH), 6.95 (d, J = 2.4, 1H, CCHCOMe), 6.77 (dd, J_1 = 9.1, J_2 = 2.4, 1H, CHC*H*OMe), 6.63 (d, J = 9.6, 1H, C*H*CHCO), 6.45 (d, J = 1.9, 1H, CCHCO), 5.96 (dd, J_1 = 9.6, J_2 = 1.9, 1H, CHC*H*CO), 4.15 (t, J = 5.2, 4H, CH_2NCS), 3.89 (s, 3H, $COOCH_3$), 3.62 (t, J = 5.2, 4H, CH_2NCO), 3.48 (s, 3H, $COCH_3$), 1.48 (s, 9H, *t*-Bu).

Piperazinyl-LRB (5). A solution of LRB sulfonyl chloride (Molecular Probes, 500 mg, 0.87 mmol) and piperazine (373 mg, 4.33 mmol) in DMF was stirred overnight under Ar. The solvent was evaporated, and flash chromatography (MeCN/MeOH/NH_4OH, 79:20:1) of the residue yielded **5** (230 mg, 0.37 mmol, 42%) as a purple powder. ^{1}H NMR (CD_3OD): δ 8.54 (d, J = 1.7, 1H, $CHCSO_3$), 8.24 (dd, J_1 = 7.9, J_2 = 1.7, 1H, CHC*H*SO$_2$), 7.56 (d, J = 7.9, 1H, C*H*CHSO$_2$), 7.09 (AB q, J = 9.5, Δ = 8.8, 4H, CHCHCN, CHC*H*CN is also coupled to CCHCN, J = 2.2), 6.98 (d, J = 2.2, 2H, CCHCN), 3.68 (q, J = 7.1, 8 H, CH_2Me), 2.90, 2.64 (two t, J = 4.8, 8H, CH_2CH_2N), 1.30 (t, J = 7.1, 12H, CH_3).

NBD-pip-COCH$_2$CH$_2$OCH$_2$C(CH$_2$OCH$_2$CH$_2$COOC$_6$Cl$_5$)$_3$ (6). DMAP (24 mg, 0.2 mmol) and **3** (50 mg, 0.20 mmol) were added to **2** (570 mg, 0.40 mmol) in THF, and the solution was stirred for 2 h. Evaporation of the solvent and flash chromatography ($CHCl_3$) yielded **6** as an orange waxy solid (157 mg, 0.112 mmol, 56%). ^{1}H NMR ($CDCl_3$): δ 8.41, 6.24 (two d, J = 8.9, 2H, ArH), 4.16, 4.01, 3.92, 3.80 (four br t, 8 H, piperazine CH_2's), 3.80 (t, J = 6.0, 6H, OCH_2CH$_2$COO), 3.75 (t, J = 6.5, 2H, OCH_2CH$_2$CON), 3.45 (s, 6H, CH_2OCH$_2$CH$_2$COO), 3.43 (s, 2H, CH_2OCH$_2$CH$_2$CON), 2.92 (t, J = 6.0, 6H, CH_2COO), 2.64 (t, J = 6.5, 2H, CH_2CON).

DiMe-FITC-pip-COCH$_2$CH$_2$OCH$_2$C(CH$_2$OCH$_2$CH$_2$COOC$_6$Cl$_5$)$_3$ (7). DMAP (27 mg, 0.22 mmol) and **4** (110 mg, 0.218 mmol) were added to **2** (618 mg, 0.436 mmol) in THF, and the solution was stirred overnight under Ar. Evaporation of the solvent and flash chromatography ($CHCl_3$/MeOH, 48:1) yielded **7** as a yellow waxy solid (75 mg, 0.045 mmol, 10%). ^{1}H NMR ($CDCl_3$): δ 9.84 (s, 1H, NH), 8.23 (d, J = 2.1, 1H, C*H*C-COOMe), 7.75 (dd, J_1 = 8.0, J_2 = 2.1, 1H, C*H*CNH), 7.10 (d, J = 9.1, 1H, C*H*CHCOMe), 7.09 (d, J = 8.0, 1H, C*H*CHCNH), 6.95 (d, J = 2.4, 1H, CCHCOMe), 6.77 (dd, J_1 = 9.1, J_2 = 2.4, 1H, CHC*H*COMe), 6.63 (d, J = 9.6, 1H, C*H*CHCO), 6.45 (d, J = 1.9, 1H, CCHCO), 5.96 (dd, J_1 = 9.6, J_2 = 1.9, 1H, CHC*H*CO), 4.26, 4.15, 3.82, 3.76 (four br t, 8 H, piperazine CH_2's), 3.80 (t, J = 6.0, 6H, CH_2CH$_2$COO), 3.75 (t, J = 6.5, 2H, CH_2CH$_2$CON), 3.46 (s, 6H, CH_2OCH$_2$CH$_2$COO), 3.44 (s, 2H, CH_2OCH$_2$CH$_2$CON), 2.92 (t, J = 6.0, 6H, CH_2COO), 2.64 (t, J = 6.5, 2H, CH_2CON).

LRB-pip-COCH$_2$CH$_2$OCH$_2$C(CH$_2$OCH$_2$CH$_2$COOC$_6$Cl$_5$)$_3$ (8). DMAP (20 mg, 0.16 mmol) and **5** (100 mg, 0.16 mmol) were added to **2** (454 mg, 0.32 mmol) in MeCN in an ice bath, and the solution was stirred overnight under Ar. Evaporation of the solvent and flash chromatography (CH_2Cl_2/ether/MeOH, 17:2:1) yielded **8** as a purple waxy solid (65 mg, 0.036 mmol, 23%). ^{1}H NMR ($CDCl_3$): δ 8.58 (s, 1H, $CHCSO_3$), 8.40 (d, J = 7.8, 1H, CHC*H*SO$_2$), 7.29 (d, J = 7.8, 1H, C*H*CHSO$_2$), 7.13 (d, J = 9.5, 2 H, C*H*CHCN), 6.87 (dd, J_1 = 9.5, J_2 = 2.3, 2H, CHC*H*CN), 6.73 (d, J = 2.3, 2H, CCHCN), 3.80 (t, J = 6.1, 6H, CH_2CH$_2$COO), 3.62 (m, 8H, CH_2CH$_2$CON + CH_2Me), 3.51, 3.36 (two br s, 8 H, piperazine CH_2's), 3.43, 3.36 (two s, 8H, CCH_2O), 2.91 (t, J = 6.1, 6H, CH_2COO), 1.34 (t, J = 7.0, 12H, CH_3).

General Procedure for Preparing Fluorescent Ferrichrome Analogues. The Boc-protective group was removed from the *N*-methylhydroxamates by stirring in TFA/CH_2Cl_2 (1:2) for 20 min and neutralized with [(diethylamino)methyl]polystyrene, which was then removed by filtration, yielding compounds **9**. *N*-Methylhydroxamates **9** (0.33 mmol) were added to THF solutions of the fluorescent-probe−piperazine−triphenolate compounds **6**, **7**, and **8** (0.10 mmol), respectively. "DMAP" on polystyrene was added to the solutions and stirred overnight. Basic pH was maintained by adding "DMAP" on polystyrene and/or [(diethylamino)methyl]-polystyrene. TLC analysis and the disappearance of the IR active ester absorption at 1783 cm^{-1} were indications that the reaction was completed. The basic polymers were removed by filtration, the filtrates were evaporated, and the residual products were purified by preparative TLC. Unless stated otherwise all compounds were obtained as viscous oils.

NBD-pip-COCH$_2$CH$_2$OCH$_2$C(CH$_2$OCH$_2$CH$_2$CONHCH$_2$CON(OH)Me)$_3$ (10G). Elution $CHCl_3$/MeOH (9:1), yield 61%. ^{1}H NMR (CD_3OD): δ 8.49, 6.53 (two d, J = 9.0, 2H, ArH), 4.28, 4.17, 3.94, 3.89 (four br t, 8H, piperazine CH_2's), 4.11 (s, 6H, $NHCH_2CO$), 3.67 (t, J = 6.2, 2H, $NCOCH_2CH_2O$), 3.61 (t, J = 6.1, 6H, $NHCOCH_2CH_2O$), 3.38, 3.36 (two s, 8H, OCH_2C), 3.17 (s, 9H, NCH_3), 2.69 (t, J = 6.2, 2H, $NCOCH_2$), 2.46 (m, 6H, $NHCOCH_2$). FABMS: 914.19 MH$^+$. UV/vis: λ_{max} 474 nm, ϵ = 27 240. Anal. ($C_{36}H_{55}N_{11}O_{17}$·2.5H_2O) C, H, N.

NBD-pip-COCH$_2$CH$_2$OCH$_2$C(CH$_2$OCH$_2$CH$_2$CONHCH-MeCON(OH)Me)$_3$ (10A). Elution $CHCl_3$/MeOH (87:13), yield 48%. ^{1}H NMR (CD_3OD): δ 8.41, 6.48 (two d, J = 8.9, 2H, ArH), 4.98 (m, 3H, CH), 4.29, 4.18, 3.99, 3.94 (four br t, 8H, piperazine CH_2's), 3.72 (t, J = 6.0, 2H, $NCOCH_2CH_2O$), 3.63 (t, J = 5.8, 6H, $NHCOCH_2CH_2O$), 3.38, 3.35 (two s, 8H, OCH_2C), 3.20 (s, 9H, NCH_3), 2.74 (t, J = 6.0, 2H, $NCOCH_2$), 2.45 (t, J = 5.8, 6H, $NHCOCH_2$), 1.32 (d, J = 7.0, 9H, $CHCH_3$). FABMS: 955.11 M$^+$. Fe(III) complex: UV/vis: λ_{max} 476 nm, ϵ = 11 920. Anal. ($C_{39}H_{61}N_{11}O_{17}$·4H_2O) C, H; N: calcd, 14.99; found, 14.31.

NBD-pip-COCH$_2$CH$_2$OCH$_2$C(CH$_2$OCH$_2$CH$_2$CONHCH(*i*-Bu)CON(OH)Me)$_3$ (10L). This compound was prepared in a slightly different manner than described in the general procedure. Compounds **2**, **3**, and **9** (R = *i*-Bu) were dissolved in THF at a 1:1:3 ratio and stirred overnight yielding **10L**, along with the dihydroxamate-diNBD and monohydroxamate-triNBD. (This procedure gave much lower yields than achieved when using the general procedure). Elution toluene/*i*-PrOH (7:3), yield 2.2%. ^{1}H NMR (CD$_3$OD): δ 8.46, 6.52 (two d, J = 9.0, 2H, ArH), 5.12 (t, J = 5.8, 3H, NHC*H*), 4.29, 4.18, 3.97, 3.92 (four br t, 8H, piperazine CH$_2$'s), 3.71 (t, J = 6.3, 2H, NCOCH$_2$C*H*$_2$O), 3.62 (m, 6H, NHCOCH$_2$C*H*$_2$O), 3.37, 3.35 (two s, 8H, OCH$_2$C), 3.18 (s, 9H, NCH$_3$), 2.73 (t, J = 6.3, 2H, NCOCH$_2$), 2.45 (m, 6H, NHCOCH$_2$), 1.69 (m, 3H, *i*-Bu CH's), 1.51 (m, 6H, *i*-Bu CH$_2$'s), 0.93 (d, J = 6.9, 18H, *i*-Bu CH$_3$'s). FABMS: 1105 MNa$^+$. UV/vis: λ_{max} 474 nm, ϵ = 14 220.

NBD-pip-COCH$_2$CH$_2$OCH$_2$C(CH$_2$OCH$_2$CH$_2$CONHCH-(Bn)CON(OH)Me)$_3$ (10P). Elution CHCl$_3$/MeOH (23:2), yield 13%. ^{1}H NMR (CD$_3$OD): δ 8.44, 6.47 (two d, J = 9.0, 2H, ArH), 7.20 (m, 15H, Ph), 5.28 (m, 3H, CH), 4.23, 4.13, 3.89, 3.89 (four br t, 8H, piperazine CH$_2$'s), 3.62 (t, J = 6.0, 2H, NCOCH$_2$C*H*$_2$O), 3.48 (t, J = 5.6, 6H, NHCOCH$_2$C*H*$_2$O), 3.22 3.20 (two s, 8H, OCH$_2$C), 3.19 (s, 9H, NCH$_3$), 2.67 (t, J = 6.0, 2H, NCOCH$_2$), 2.36 (t, J = 5.6, 6H, NHCOCH$_2$). FABMS: 1181.66 (M − H$_2$)$^+$. UV/vis: λ_{max} 481 nm, ϵ = 22 580.

DiMe-FITC-pip-COCH$_2$CH$_2$OCH$_2$C(CH$_2$OCH$_2$CH$_2$CONH-CH$_2$CON(OH)Me)$_3$ (11G). Elution CHCl$_3$/MeOH (17:3), yield 21%. ^{1}H NMR (CD$_3$OD): δ 8.54 (br s, 1H, NHCS), 8.31 (d, J = 2.1, 1H, CHCCOOMe), 7.86 (dd, J_1 = 8.2, J_2 = 2.1, 1H, C*H*CNH), 7.36 (d, J = 8.2, 1H, C*H*CHCNH), 7.25 (d, J = 2.4, 1H, CCHCOMe), 7.20 (d, J = 9.0, 1H, C*H*CHCOMe), 7.18 (d, J = 9.6, 1H, C*H*CHCO), 6.96 (dd, J_1 = 9.0, J_2 = 2.4, 1H, CHC*H*OMe), 6.60 (dd, J_1 = 9.6, J_2 = 2.0, 1H, CHC*H*CO), 6.51 (d, J = 2.0, 1H, CCHCO), 4.16 (s, 6H, C*H*$_2$CONOH), 4.14 (br d, 4H, CH$_2$NCS), 3.99 (s, 3H, COOCH$_3$), 3.83 (m, 4H, CH$_2$-NCO), 3.71 (t, J = 6.1, 2H, C*H*$_2$CH$_2$CON), 3.67 (t, J = 6.0, 6H, C*H*$_2$CH$_2$CONH), 3.60 (s, 3H, COCH$_3$), 3.42 (s, 8H, CCH$_2$O), 3.21 (s, 9H, NCH$_3$), 2.72 (t, J = 6.1, 2H, CH$_2$CON), 2.52 (t, J = 6.0, 6H, C*H*$_2$CONH). FABMS: 1169.12 MH$^+$. Fe(III) complex: UV/vis: λ_{max} 458 nm, ϵ = 8864.

DiMe-FITC-pip-COCH$_2$CH$_2$OCH$_2$C(CH$_2$OCH$_2$CH$_2$CONH-CHMeCON(OH)Me)$_3$ (11A). Elution CHCl$_3$/MeOH (9:1), yield 37%. ^{1}H NMR (CD$_3$OD): δ 8.30 (d, J = 2.1, 1H, CHCCOOMe), 7.86 (dd, J_1 = 8.2, J_2 = 2.1, 1H, C*H*CNH), 7.35 (d, J = 8.2, 1H, C*H*CHCNH), 7.24 (d, J = 2.4, 1H, CCHCOMe), 7.19 (d, J = 9.0, 1H, C*H*CHCOMe), 7.16 (d, J = 9.6, 1H, C*H*CHCO), 6.95 (dd, J_1 = 9.0, J_2 = 2.4, 1H, CHC*H*COMe), 6.59 (dd, J_1 = 9.6, J_2 = 2.0, 1H, CHC*H*CO), 6.50 (d, J = 2.0, 1H, CCHCO), 5.00 (t, J = 7.0, 3H, CHMe), 4.18, 4.07 (two br t, 4H, CH$_2$NCS), 3.98 (s, 3H, COOCH$_3$), 3.82 (m, 4H, CH$_2$NCO), 3.71 (t, J = 6.1, 2H, C*H*$_2$CH$_2$CON), 3.64 (t, J = 6.0, 6H, C*H*$_2$-CH$_2$CONH), 3.59 (s, 3H, COCH$_3$), 3.40, 3.39 (two s, 8H, CCH$_2$O), 3.20 (s, 9H, NCH$_3$), 2.71 (t, J = 6.1, 2H, CH$_2$CON), 2.46 (t, J = 5.6, 6H, C*H*$_2$CONH), 1.32 (d, J = 7.0, 9H, CHC*H*$_3$). FABMS: 1210.18 M$^+$. UV/vis: λ_{max} 457 nm, ϵ = 16 040.

LRB-pip-COCH$_2$CH$_2$OCH$_2$C(CH$_2$OCH$_2$CH$_2$CONHCH$_2$-CON(OH)Me)$_3$ (12G). Elution CHCl$_3$/MeOH (17:3), yield 81%. ^{1}H NMR (CD$_3$OD): δ 8.54 (d, J = 1.5, 1H, CHCSO$_3$), 8.27 (dd, J_1 = 7.9, J_2 = 1.5, 1H, CHC*H*SO$_2$), 7.59 (d, J = 7.9, 1H, C*H*CHSO$_2$), 7.11 (AB q, J = 9.5, Δ = 10.2, 4 H, CHCHCN, CHC*H*CN also coupled to CCHCN, J = 2.1), 6.98 (d, J = 2.1, 2H, CCHCN), 4.15 (s, 6H, C*H*$_2$CONOH), 3.69 (q, J = 7.0, 8H, C*H*$_2$Me), 3.63 (t, J = 6.0, 8H, CH$_2$C*H*$_2$O), 3.47, 3.43 (two br m, 4H, SO$_2$NCH$_2$ {piperazine}), 3.36, 3.35 (two s, 8H, CCH$_2$O), 3.20 (s, 9H, NCH$_3$), 3.15, 2.95 (two br m, 4H, CH$_2$NCO {piperazine}), 2.53 (t, J = 6.0, 2H, NCOC*H*$_2$CH$_2$O), 2.43 (t, J = 6.0, 6H, NHCOC*H*$_2$CH$_2$O), 1.32 (t, J = 7.0, 12H, CH$_2$C*H*$_3$). FABMS: 1290.83 M$^+$, 1312.81 MNa$^+$. Anal. (C$_{57}$H$_{82}$N$_{10}$O$_{20}$S$_2$·10H$_2$O) C, H, N.

LRB-pip-COCH$_2$CH$_2$OCH$_2$C(CH$_2$OCH$_2$CH$_2$CONHCH-MeCON(OH)Me)$_3$ (12A). Elution CHCl$_3$/MeOH (22:3), crystallized from EtOH/hexane, yield 69%, mp 135 °C. ^{1}H NMR (CD$_3$OD): δ 8.54 (d, J = 1.4, 1H, CHCSO$_3$), 8.27 (dd, J_1 = 7.8, J_2 = 1.5, 1H, CHC*H*SO$_2$), 7.59 (d, J = 7.8, 1H, C*H*CHSO$_2$), 7.09 (AB q, J = 9.5, Δ = 10.2, 4 H, CHCHCN, CHC*H*CN also coupled to CCHCN, J = 2.0), 6.98 (d, J = 2.0, 2H, CCHCN), 5.01 (m, 3H, C*H*CONOH), 3.68 (q, J = 7.1, 8H, C*H*$_2$Me), 3.61, 3.60 (m, 8H, CH$_2$C*H*$_2$O), 3.50, 3.45 (two br t, 4H, SO$_2$NCH$_2$ {piperazine}), 3.34, 3.33 (two s, 8H, CCH$_2$O), 3.19 (s, 9H, NCH$_3$), 3.05, 2.92 (two br t, 4H, CH$_2$NCO {piperazine}), 2.58 (t, J = 7.0, 2H, NCOC*H*$_2$CH$_2$O), 2.43 (m, 6H, NHCOC*H*$_2$CH$_2$O), 1.30 (m, 21H, CH$_2$C*H*$_3$ + CHC*H*$_3$). FABMS: 1356.75 (MH-Na)$^+$. Anal. (C$_{60}$H$_{88}$N$_{10}$O$_{20}$S$_2$·5H$_2$O) C, H; N: calcd, 9.84; found, 7.86.

LRB-pip-COCH$_2$CH$_2$OCH$_2$C(CH$_2$OCH$_2$CH$_2$CONHCH(*i*-Bu)CON(OH)Me)$_3$ (12L). Elution CHCl$_3$/MeOH (9:1), 10% yield. This compound was prepared by using the procedure described for compound **10L** and not by the general procedure. ^{1}H NMR (CD$_3$OD): δ 8.54 (d, J = 1.5, 1H, CHCSO$_3$), 8.27 (dd, J_1 = 7.8, J_2 = 1.5, 1H, CHC*H*SO$_2$), 7.59 (d, J = 7.8, 1H, C*H*CHSO$_2$), 7.09 (AB q, J = 9.5, Δ = 13.5, 4 H, CHCHCN, CHC*H*CN is also coupled to CCHCN J = 2.2), 6.97 (d, J = 2.2, 2H, CCHCN), 5.13 (t, J = 6.9, 3H, C*H*CONOH), 3.67, 3.63, 3.61 (m, 16H, C*H*$_2$Me + CH$_2$C*H*$_2$O), 3.42 (br t, 4H, SO$_2$NCH$_2$-{piperazine}), 3.37, 3.36 (two s, 8H, CCH$_2$O), 3.20 (s, 9H, NCH$_3$), 3.05, 2.92 (two br t, 4H, CH$_2$NCO {piperazine}), 2.60 (t, J = 6.2, 2H, NCOC*H*$_2$CH$_2$O), 2.48 (t, J = 6.0, 6H, NHCOC*H*$_2$CH$_2$O), 1.70 (m, 3H, *i*-Bu CH's), 1.53 (dd, J = 6.9, 6H, *i*-Bu CH$_2$'s), 1.30 (t, J = 6.9, 12H, CH$_2$C*H*$_3$), 0.95 (d, J = 6.6, 18H, *i*-Bu CH$_3$'s). FABMS: 1427.3 (M − O$_2$)$^+$. UV/vis: λ_{max} 556 nm, ϵ = 52 800.

Bacterial Strains. The sid$^-$ mutants *P. putida* JM218, *P. fluorescens* S680 and *P. fluorescens* WCS 3742 were kindly provided by L. C. van Loon, Utrecht, The Netherlands.

In Vivo Fluorescence Studies. The bacteria were grown in LMKB medium[42] overnight at 28 °C on a rotary shaker at 180 rpm. Bacterial cultures were centrifuged for 15 min at 2500 rpm, resuspended in fresh half-strength standard succinate medium (SSM) to a final absorbance of 0.6 (at 620 nm), and incubated for 60 min at 28 °C. In some experiments NaN_3 was added 30 min prior to the addition of the siderophores to a final concentration of 5 mM. The Fe−siderophore complexes were added to the bacterial suspensions to a final concentration of 1 or 5 μM. Aliquots of 1 mL were centrifuged, and the supernatants were collected. Experiments were performed in duplicate.

Growth Curve Studies. The 100 mL flasks were washed with 6 N HCl followed by thorough rinsing with double-distilled water, prior to autoclaving, and filled with 10 mL of Chelite-treated SSM. Fe−siderophores were added to a final concentration of 1 μM. The flasks were inoculated with bacteria and shaken on a rotary shaker at 180 rpm at 28 °C. Samples were taken at specific intervals, and turbidity and absorbance at λ = 620 nm were recorded. Experiments were performed in duplicate.

Acknowledgment. The authors thank Mrs. Rahel Lazar for her skillful technical assistance. Financial support from the U.S.−Israel Binational Science Foundation, the Dutch−Israeli Agricultural Research Program (DIARP), the Minerva Foundation, and the Israel Academy of Sciences and Humanities is greatly acknowledged. A. Shanzer is holder of the Singfried and Irma Ullman Professorial Chair.

References

(1) Weizman, H.; Ardon, O.; Mester, B.; Libman, J.; Dwir, O.; Hadar, Y.; Chen, Y.; Shanzer, A. Fluorescently-Labeled Ferrichrome Analogs as Probes for Receptor-Mediated, Microbial Iron Uptake. *J. Am. Chem. Soc.* **1996**, *118*, 12368−12375.

(2) Neilands, J. B.; Konopka, K.; Schwyn, B.; Coy, M.; Fransis, R. T.; Paw, B. H.; Bagg, A. Comparative Biochemistry of Microbial Iron Assimilation. In *Iron Transport in Microbes, Plants and Animals*; Winkelmann, G., van der Helm, D., Neilands, J. B., Eds.; VCH: Weinheim, 1987; pp 3−33.

(3) Neilands, J. B. Microbial Iron Compounds. *Annu. Rev. Biochem.* **1981**, *50*, 715−731.

(4) Raymond, K. N.; Mueller, G.; Matzanke, B. F. Complexation of Iron by Siderophores. A Review of Their Solution and Structural Chemistry and Biological Function. *Top. Curr. Chem.* **1984**, *123*, 49−102.
(5) Glynn, A. A. Bacterial Factors Inhibiting Host Defence Mechanisms. *Sym. Soc. Gen. Microbiol.* **1972**, *22*, 75−112.
(6) Rogers, H. J. Iron-Binding Catechols and Virunlece in *Escherichia coli*. *Infect. Immun.* **1973**, *7*, 445−456.
(7) Neilands, J. B. Siderophores: Structure and Function of Microbial Iron Transport Compounds. *J. Biol. Chem.* **1995**, *270*, 26723−26726.
(8) Crowley, D. E.; Wang, Y. C.; Reid, C. P. P.; Szaniszlo, P. J. Mechanisms of Iron Acquisition from Siderophores by Microorganisms and Plants. In *Iron Nutrition and Interactions in Plants*; Chen, Y., Hadar, Y., Eds.; Kluwer Academic Publishers: Netherlands, 1991; pp 213−232.
(9) Wayne, R.; Neilands, J. B. Evidence for Common Binding Sites for Ferrichrome Compounds and Bacteriophage phi 80 in the Cell Envelope of Escherichia coli. *J. Bacteriol.* **1975**, *121*, 497−501.
(10) Killmann, H.; Benz, R.; Braun, V. Conversion of the FhuA Transport Protein into a Diffusion Channel Through the Outer Membrane of *Escherichia coli*. *EMBO J.* **1993**, *12*, 3007−3016.
(11) Killmann, H.; Benz, R.; Braun, V. Properties of the FhuA Channel in the *Escherichia coli* Outer Membrane after Deletion of FhuA Portions within and outside the Predicted Gating Loop. *J. Bacteriol.* **1996**, *178*, 6913−6920.
(12) Rutz, J. M.; Liu, J.; Lyons, J. A.; Goranson, J.; Armstrong, S. K.; Mcintosh, M. A.; Feix, J. B.; Klebba, P. E. Formation of a Gated Channel by a Ligand-Specific Transport Protein in the Bacterial Outer Membrane. *Science* **1992**, *258*, 471−475.
(13) Jiang, X.; Payne, M. A.; Cao, Z.; Foster, S. B.; Feix, J. B.; Newton, S. M. C.; Klebba, P. E. Ligand-Specific Opening of a Gated-Porin Channel in the Membrane of Living Bacteria. *Science* **1997**, *276*, 1261−1264.
(14) Jurkevitch, E.; Hadar, Y.; Chen, Y.; Libman, J.; Shanzer, A. Iron Uptake and Molecular Recognition in *Pseudomonas putida*: Receptor Mapping with Ferrichrome and its Biomimetic Analogs. *J. Bacteriol.* **1992**, *174*, 78−83.
(15) Bodenant, B.; Fages, F. Synthesis, Metal Binding, and Fluorescence Studies of a Pyrene-tethered Hydroxamic Acid Ligand. *Tetrahedron Lett.* **1995**, *36*, 1451−1454.
(16) Fages, F.; Bodenant, B.; Weil, T. Fluorescent, Siderophore-Based Chelators. Design and Synthesis of a trispyrenyl Trishydroxamate Ligand, an Intramolecular Eximer-Forming Sensing Molecule Which Responds to Iron(III) and Gallium(III) Metal Cations. *J. Org. Chem.* **1996**, *61*, 3956−3961.
(17) Sohna, J.-E. S.; Fages, F. Sensitized Luminescence Emission of the Europium(III) Ion Bound to a Pyrene-Containing Triacid Ligand. *Tetrahedron Lett.* **1997**, *38*, 1381−1384.
(18) Lytton, S. D.; Cabantchik, Z. I.; Libman, J.; Shanzer, A. Reversed siderophores as antimalarial agents. II. Selective scavenging of Fe(III) from parasitized erythrocytes by a fluorescent derivative of desferal. *Mol. Pharmacol.* **1991**, *40*, 584−590.
(19) Lytton, S. D.; Mester, B.; Libman, J.; Shanzer, A.; Cabantchik, Z. I. Monitoring of Iron(III) Removal from Biological Sources Using a Fluorescent Siderophore. *Anal. Biochem.* **1992**, *205*, 326−333.
(20) Bar-Ness, E.; Hadar, Y.; Chen, Y.; Shanzer, A.; Libman, J. Iron Uptake by Plants from Microbial Siderophores. *J. Plant Physiol.* **1992**, *99*, 1329−1335.
(21) Weizman, H. Helical Complexes for the Study of Light Induced Electron Transfer Processes. M. Sc. Thesis, Weizmann Institute of Science, 1994.
(22) Ardon, O.; Weizman, H.; Libman, J.; Shanzer, A.; Chen, Y.; Hadar, Y. Iron Uptake in *Ustilago maydis*: Studies with Fluorescent Ferrichrome Analogues. *Microbiology* **1997**, *143*, 3625−3631.
(23) Ardon, O.; Nudelman, R.; Libman, J.; Shanzer, A.; Chen, Y.; Hadar, Y., *J. Bacteriol.* **1998**, *180*, in press.
(24) Shanzer, A.; Libman, J.; Yakirevitch, P.; Hadar, Y.; Chen, Y.; Jurkevitch, E. Siderophore-Mediated Microbial Iron(III) Uptake: An Exercise in Chiral Recognition. *Chirality* **1993**, *5*, 359−365.
(25) The hydrophobic ferrichrome analogues permeate across erythrocytic membranes and behave as intracellular iron scavengers, thereby acting as growth inhibitors. This is in contrast to natural carriers, which participate in receptor-mediated iron uptake in cells and act as growth promoters.
(26) Shanzer, A.; Libman, J.; Lytton, S. D.; Glickstein, H.; Cabantchik, Z. I. Reversed Siderophores Act as Antimalarial Agents. *Proc. Natl. Acad. Sci. U.S.A.* **1991**, *88*, 6585−6589.
(27) Corrie, J. E. T.; Trentham, D. R. Synthesis of Photoactive Fluorescein Derivatives Bearing Side Chains with Varying Properties. *J. Chem. Soc., Perkin Trans. 1* **1995**, 1993−2000.
(28) Donckt, E. V.; Vooren, C. V. Electron Transfer from Aromatic Molecules to Dimethylmercury via a Triplet Exciplet. *J. Chem. Soc., Faraday Trans. 1* **1978**, *74*, 827−836.
(29) Loyevsky, M.; Lytton, S. D.; Mester, B.; Libman, J.; Shanzer, A.; Cabantchik, Z. I. The Antimalarial Action of Desferal Involves a Direct Access Route to Erythrocytic (*Plasmodium falciparum*) Parasites. *J. Clin. Invest.* **1993**, *91*, 218−224.
(30) Bissell, R. A.; de Silva, A. P.; Gunaratne, H. Q. N.; Lynch, P. L. M.; Maguire, G. E. M.; Sandanayake, K. R. A. S. Molecular Fluorescent Signaling with "Fluor-Spacer-Receptor' Systems: Approaches to Sensing and Switching Devices via Supramolecular Photophysics. *Chem. Soc. Rev.* **1992**, *21*, 187−195.
(31) Birks, J. B. *Photophysics of Aromatic Molecules*; Wiley-Interscience: London, New York, Sydney, Toronto, 1970.
(32) Jurkevich, E.; Hadar, Y.; Chen, Y. Differential Siderophore Utilization and Iron Uptake by Soil and Rhizosphere Bacteria. *Appl. Environ. Microbiol.* **1992**, *58*, 119−124.
(33) Berner, I.; Winkelmann, G. Ferrioxamine Transport Mutants and the Identification of the Ferrioxamine Receptor Protein (Fox A) in *Erwinia herbicola (Enterobacter agglomerans). Biol. Metals* **1990**, *2*, 197−202.
(34) Jurkevitch, E.; Hadar, Y.; Chen, Y.; Yakirevitch, P.; Libman, J.; Shanzer, A. Iron Uptake and Molecular Recognition in *Pseudomonas putida*: Receptor Mapping with Ferrioxamine B, Coprogen B and Their Biomimetic Analogues. *Microbiology* **1994**, *140*, 1697−1703.
(35) Shanzer, A.; Libman, J. Biomimetic Siderophores. In *Handbook of Microbial Iron Chelates*; Winkelmann, G., Ed.; CRC Press: Boca Raton, FL, 1991; pp 309−338.
(36) Berner, I.; Yakirevitch, P.; Libman, J.; Shanzer, A.; Winkelmann, G. Chiral Linear Hydroxamates as Biomimetic Analogues of Ferrioxamine and Coprogen and Their Use in Probing Siderophore-Receptor Specificity in Bacteria and Fungi. *Biology of Metals* **1991**, *4*, 186−191.
(37) Shanzer, A.; Libman, J. From Biomimetic Ion Carriers to Helical Structures. *Croat. Chem. Acta* **1996**, *69*, 709−729.
(38) Shanzer, A.; Libman, J. Biomimetic Siderophores: From Structural Probes to Diagnostic Tools. In *Iron Transport and Storage in Microorganisms, Plants, and Animals*; Sigel, A., Sigel, H., Eds.; Marcel Dekker: New York, 1998; Vol. 35 of "Metal Ions in Biological Systems"; pp 329−354.
(39) Sharma, S. K.; Miller, M. J.; Payne, S. M. Spermexatin and Spermexatol: New Synthetic Spermidine-Based Siderophore Analogues. *J. Med. Chem.* **1989**, *32*, 357−367.
(40) Dolence, E. K.; Lin, C. E.; Miller, M. J. Synthesis and Siderophore Activity of Albomycin-like Peptides Derived from N^5-Acetyl-N^5-L-ornithine. *J. Med. Chem.* **1991**, *34*, 956−968.
(41) Dayan, I.; Libman, J.; Agi, Y.; Shanzer, A. Chiral Siderophore Analogs: Ferrichrome. *Inorg. Chem.* **1993**, *32*, 1467−1475.
(42) King, E. O.; Ward, M. K.; Raney, D. E. Two Simple Media for the Demonstration of Pyocyanin and Fluorescin. *J. Lab. Clin. Med.* **1954**, *44*, 301−307.

JM970581B